ELSEVIER

Chemosphere 65 (2006) 1784–1790

CHEMOSPHERE

www.elsevier.com/locate/chemosphere

Dose-controlled exposure of A549 epithelial cells at the air–liquid interface to airborne ultrafine carbonaceous particles

E. Bitterle [a,b], E. Karg [a], A. Schroeppel [a], W.G. Kreyling [a,b], A. Tippe [a], G.A. Ferron [a], O. Schmid [a], J. Heyder [a], K.L. Maier [a,c,*], T. Hofer [a,c]

[a] *GSF National Research Center for Environment and Health, Institute for Inhalation Biology, Ingolstaedter Landstr. 1, D-85764 Neuherberg/Munich, Germany*

[b] *GSF Focus-Network Aerosols and Health, GSF-Institute for Inhalation Biology and Asklepios Clinics GmbH Muenchen-Gauting, Germany*

[c] *Clinical Cooperation Group Inflammatory Lung Diseases, GSF-Institute for Inhalation Biology and Asklepios Clinics GmbH Muenchen-Gauting, Germany*

Received 5 October 2005; received in revised form 3 April 2006; accepted 11 April 2006
Available online 9 June 2006

Abstract

The geometry of commercially available perfusion chambers designed for harbouring three membrane-based cell cultures was modified for reliable and dose-controlled air–liquid interface (ALI) exposures. Confluent A549 epithelial cells grown on membranes were integrated in the chamber system and supplied with medium from the chamber bottom. Cell viability was not impaired by the conditions of ALI exposure without particles. Expression of the inflammatory cytokines interleukin 6 and interleukin 8 by A549 cells during ALI exposure to filtered air for 6 h and subsequent stimulation with tumor necrosis factor was not altered compared to submersed controls, indicating that the cells maintained their functional integrity. Ultrafine carbonaceous model particles with a count median mobility diameter of about 95 ± 5 nm were produced by spark discharge at a stable concentration of about 2×10^6 cm^{-3} and continuously monitored for accurate determination of the exposure dose. Delivery to the ALI exposure system yielded a homogeneous particle deposition over the membranes with a deposition efficiency of 2%. Mid dose exposure of A549 cells to this aerosol for 6 h yielded a total particle deposition of $(2.6 \pm 0.4) \times 10^8$ cm^{-2} corresponding to (87 ± 23) ng cm^{-2}. The 2.7-fold ($p \leqslant 0.05$) increased transcription of heme oxygenase-1 indicated a sensitive antioxidant and stress response, while cell viability did not reveal a toxic mechanism.

Keywords: In vitro exposure system; Interleukin 6; Interleukin 8; Heme oxygenase-1; Ultrafine particles

1. Introduction

Ambient concentrations of fine and ultrafine particulates (ufp) are associated with respiratory effects (Peters et al., 1997). These particles are deposited very efficiently in the lung periphery and might elicit adverse responses (Oberdorster et al., 2000; Donaldson et al., 2002). Ufp contribute little to particle mass but dominate particle number of ambient aerosols. Adverse effects of ufp on target cells are influenced by size-dependent binding and uptake. Recent data indicate that ufp easily penetrate into the cell membrane of non-phagocytic cells such as human red blood cells (Rothen-Rutishauser et al., 2004) and alveolar type II epithelial cells (Griese and Reinhardt, 1998). Several studies indicate an increased toxic potential of ufp compared to larger particles (Reibman et al., 2002; Choi et al., 2004; Renwick et al., 2004). For a given chemical composition, a correlation between particle size and biological endpoints such as membrane integrity, interleukin 6 (IL-6) and interleukin 8 (IL-8) release is shown in human macrophages and epithelial cells by Wottrich et al. (2004).

* Corresponding author. Tel.: +49 89 3187 2319; fax: +49 89 3187 2809.
E-mail address: kmaier@gsf.de (K.L. Maier).

0045-6535/$ - see front matter © 2006 Elsevier Ltd. All rights reserved.
doi:10.1016/j.chemosphere.2006.04.035

Hence, both particle number concentration and size are toxicologically important parameters.

Diesel exhaust particles as a major source of ufp cause immunological effects in submersed cultures of macrophages (Li et al., 2000, 2002; Hofer et al., 2004). Foster et al. (2001) and Stearns et al. (2001) showed that A549 cells can internalize microspheres and aggregates of ufp, respectively. It is concluded from in vitro studies that particle exposure of lung epithelial cells might initiate inflammatory mechanisms (Bayram et al., 1998; Abe et al., 2000).

Exposure of submersed cells to suspended particles is a classical procedure to study particle effects on inflammatory pathways. For this experimental approach, particle concentrations between 10 and 200 μg/ml are often applied, which appears to be far above a realistic exposure dose. In addition, it is unknown which fraction of the suspended particles will interact with submersed cells cultured as monolayer.

As a more realistic approach, Abe et al. (2000) exposed bronchial epithelial cells cultured at the ALI to freshly produced diesel exhaust particles. They found an increased production of the cytokine IL-8 that was attributed to the soot particles. However, despite their efforts to monitor the concentration of the exhaust particles, the deposited fraction was unknown and, hence, no information on exposure dose was obtained. Aufderheide et al. (2001) described an exposure facility, known as the CULTEX system, which was supplemented with tops (Ritter et al., 2001) for exposure at the ALI. For studies with cigarette smoke, the particle concentration was determined by a light scattering method, while the particle size distribution was not assessed. Exposure of HFBE21 cells to synthetic air and smoke with and without particle filtration revealed that cell viability was less reduced by whole smoke than by filtered smoke exposure of the cells. The authors concluded that the particles had a cell-protecting effect. As a methodological add-on of the CULTEX system, Ritter et al. (2003) described a fluorimetric determination of particle deposition on membranes in separate runs without cells. Cheng et al. (2003) described an exposure technique at the ALI using transwell membranes to study biological effects of diluted exhaust from diesel and gasoline powered engines on A549 cells. With this approach, the effects on IL-8 expression of TNF primed cells were found to be stronger for gasoline engines. However, no exposures were performed with filtered exhaust to discriminate between effects mediated by the gaseous and the particulate phase. Again, only the particle size distribution in the exhaust was measured, but no information on the deposited particle fraction and, hence, the exposure dose was available.

In our approach, an ALI exposure system for airborne particles was designed, that provides a homogeneous and quantifiable deposition of the particles based on the well-characterized particle deposition in a stagnation point aerosol flow (Tippe et al., 2002). Using this technology, 2% of the aerosol particles are deposited uniformly on cell-covered membranes permitting aerosol exposure measurements with reliable particle dosimetry (Tippe et al., 2002). The system was tested by exposing A549 cells as model of alveolar epithelial cells to ultrafine carbonaceous particles. As indicator for biological response the transcription of genes like heme oxygenase-1 (HO-1), IL-6 and IL-8 was monitored.

2. Methods

2.1. Exposure chamber

A commercially available perfusion unit (MINUCELL, Bad Abbach, Germany) was adapted to study biological effects of fine and ultrafine particles (75–1000 nm) on cultured cells. The setup is a scaled-up version of the one described by Tippe et al. (2002) that increases the quantity of exposed cells to 3×10^7 cells by using a 47 mm instead of a 6 mm membrane. To maintain the same flow conditions and hence the same particle deposition efficiency the geometry was scaled up by leaving the Reynolds number constant at 6.3. The scaling led to 24 mm for the diameter of the inflow tube, 4 mm distance between tube end and membrane, and a volume flow of 250 ml min^{-1}.

The radially symmetric stagnation point flow arrangement deposits particles uniformly and quantifiably onto a circular membrane (cell layer). Due to the low flow velocity over the membrane, the mechanisms of particle deposition are (1) convective transport and (2) diffusion (Tippe et al., 2002). It will be shown below that the scaled-up chamber design resulted in the same particle deposition characteristics as the original chamber. For ALI exposure of epithelial cells with ufp, three exposure units (membrane dishes) in parallel were connected to the aerosol and medium supply. Special care was taken to provide identical aerosol concentrations to each of these units using a flow distributor that allowed for symmetric flow splitting.

For cell exposures, Anodisc membranes (Whatman, Maidstone, UK) with 47 mm diameter and a pore size of 0.2 μm were used. These membranes remained completely plane after humidification, which was important for homogeneous medium transport from the lower compartment and for homogenous particle deposition during exposure. In addition, the wetted membranes became transparent which allowed microscopic examinations of cell layers during culture by light microscopy.

2.2. Aerosol production and characterization

A schematic view of the experimental setup of the exposure system is shown in Fig. 1. In this study ultrafine carbonaceous particles (C-ufp) were produced with a spark discharge aerosol generator (GFG 1000, Palas, Karlsruhe, Germany) operated at a volumetric flow rate of 6 l min^{-1} pure argon (Ar) (purity of 99.999%) and a spark frequency of 240 Hz using graphite rods (RW0, SGL Carbson AG, Bonn, Germany; less than 0.2 ppm metal contamination).

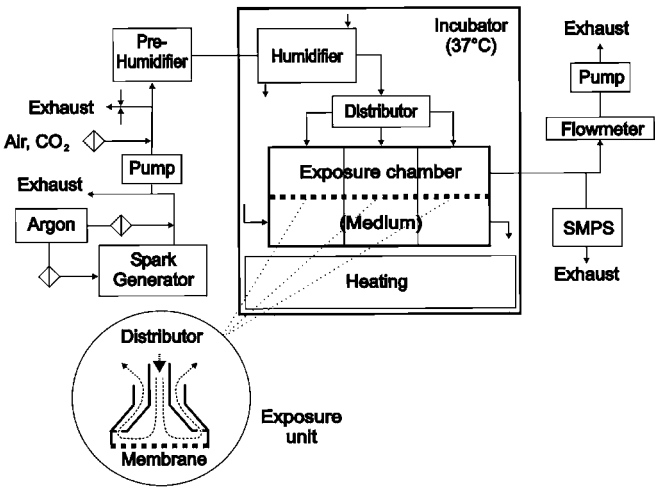

Fig. 1. Schematic of the experimental setup.

To reduce particle coagulation the aerosol was diluted (1:1) with Ar directly after generation. The particle size distribution between 16 and 673 nm (diameter) was measured with a scanning mobility particle sizer (SMPS, Model 3080, TSI Inc., St. Paul, MN, USA) and a condensation particle counter (CPC; Model 3025A, TSI Inc., St. Paul, MN, USA). The mass specific surface area of these particles was 750 $m^2\,g^{-1}$ as determined by the standard method described by Brunauer, Emmett, and Teller (BET) (Brunauer et al., 1938; Roth et al., 2004). In addition, the C-ufp showed a pronounced oxidative potential (Beck-Speier et al., 2005).

2.3. Aerosol dilution and humidification

An aerosol flow rate of 1 l min^{-1} was taken by a peristaltic pump and diluted with 10 l min^{-1} of filtered laboratory air mixed with 5% CO_2. The humidity was adjusted for exposure conditions in two steps: (i) increasing the temperature to around 30 °C and pre-humidification in a water saturated glass bulb vessel and (ii) adjusting to 36.5 ± 1 °C and final humidification to RH = 99.5% by passing the sample through a glass tube of 3 cm diameter covered with tissue paper saturated with a physiological salt solution. Based on theoretical considerations, the temperature and the relative humidity differ by less than 0.1% from its final wall value (Ferron et al., 1985). The final humidifier and the exposure chambers were placed inside an incubator at 36.5 ± 1 °C. The sample flow was controlled by a pump (DC12/08 NK, FuerGut, Tannheim, Germany).

2.4. Cell cultures

A549 cells from a human lung adenocarcinoma showing the alveolar type II phenotype were obtained from ATTC (Manassas, VA, USA). Cells were cultured in DMEM-F12 (31330-038, Gibco, Karlsruhe) supplemented with 10% fetal calf serum (S0115, Biochrom, Berlin), penicillin 100 U ml^{-1} and streptomycin 100 μg ml^{-1} (15140-114, Gibco) in a humidified atmosphere containing 5% CO_2 at 37 °C.

For the membrane-based cultures, 2×10^6 cells (passage # 31–53) were seeded in 2 ml DMEM-F12 on Anodisc membranes in 10 ml medium and allowed to adhere for 2 h. Another 10 ml of medium was added for culturing the cells on the membranes under submersed conditions and a 10 ml medium aliquot was exchanged every 3–4 days.

In a pre-study, cell growth on Anodisc membranes was monitored over 12 days. At days 6, 8, 10 and 12 of culture, cells were fixed on the Anodisc with 4% formaldehyde and subsequently stained with mouse anti-actin (A4700, Sigma, Taufkirchen, Germany) and anti-β-tubulin (T4026, Sigma) antibodies by a FITC conjugated secondary anti-mouse antibody (F0257, Sigma). The membranes were cut into 5 pieces, embedded into Antifade (P-7481, Molecular Probes, Leiden, Netherlands) and studied by confocal laser scanning microscopy (LSM 410, Zeiss, Jena, Germany) to monitor formation of a confluent monolayer. After 10 days of culture, monolayer formation was optimal, while multilayer formation was still low. There are contrary reports on the functional integrity of A549 monolayers. Foster et al. (1998) and Kim et al. (2001) described the absence of functional tight junctions in A549 cultures not forming confluent monolayers, while Rothen-Rutishauser et al. (2005) reported on the formation of tight junctions in the monolayers together with development of transepithelial electrical resistance and polarization into apical and basolateral domains.

Before each exposure experiment all membranes were examined microscopically for confluency of the cell layer, and membranes with inhomogenous cell growth were sorted out.

2.5. Exposure protocol

For exposure at the ALI, Anodisc membranes with A549 cells showing confluent monolayers after 10 days were integrated in exposure chambers (Fig. 1) each consisting of three parallel exposure units and supplied with medium from the bottom-site with a flow rate of 80 ml h^{-1}. Cells in one chamber were exposed to the aerosol under controlled conditions for 6 h, respectively, while cells in a second chamber were exposed to a control atmosphere. The control atmosphere (clean air) was obtained by filtration of one branch of a splitted aerosol flow using a PALL filter (BB50TE, PALL, Newquay, UK). More than 99.9% of particles could be removed resulting in particle number concentrations $<1 \times 10^2\,cm^{-3}$. For studying changes of HO-1 gene expression after particle exposure, three dose intervals were compared in 4–6 independent exposures: as described in detail below the total mass of deposited particles per cm^2 cell monolayer surface during 6 h of exposure was 44 ± 4 ng as low dose, 87 ± 23 ng as mid dose and 230 ± 70 ng as high dose. For IL-6 and IL-8 expression

studies, only cells exposed to mid doses of particles were considered.

2.6. Post-exposure treatment

After finishing exposure, the Anodisc membranes with the cells were incubated under submersed conditions for 1 h in absence/presence of 30 ng ml^{-1} tumor necrosis factor (TNF) in 3 ml medium to assess responsiveness to a strong inflammatory stimulus. Thereafter, cells were washed with PBS and detached from the Anodisc by adding 800 µl of trypsin/EDTA 0.25% solution below and 800 µl on the top of the membrane and incubated for 4 min at 37 °C. Trypsination was stopped with 6 ml of FCS containing medium and cells were scrapped off from the membrane afterwards. After centrifugation, the cells were resuspended in PBS and the cell number was determined after staining with *trypan blue*.

2.7. Viability assay (total reductive capacity by WST-1 reduction)

To test viability of cultured cells the proliferation assay WST-1 (1644807, Roche Diagnostics, Mannheim) was applied. The confluent cell layers on the membranes were inserted into the chambers and exposed at the ALI in absence (clean air) or presence of airborne particles and cell viability was compared with that of a submersed cell culture as control. Formazan formation by reductive cleavage was measured photometrically (Cook and Mitchell, 1989; Knebel et al., 1998).

2.8. Functional assay: IL-6, IL-8 and HO-1 transcription

To study the impact of changed culture conditions or the effect of ufp on gene expression during cell exposure, transcript levels of IL-6, IL-8 and HO-1 were measured by real-time PCR. The results after particle exposure were normalized to baseline levels.

Total RNA was extracted from A549 by using Tri-Reagent (T9424, Sigma). To assist the precipitation, 15 µg tRNA and 20 µg glycogen type IX (G0885, Sigma) were added. After isolation the RNA was reverse transcribed with oligo (dT) as primer. Polymerase chain reaction was performed according to the method of Wang et al. (1989). Quantitative PCR was performed using the LightCycler system (Roche Diagnostics, Mannheim, Germany). Three µl of cDNA were used for amplification in the SYBR Green format using the LightCycler-FastStart DNA Master SYBR Green I kit from Roche (2239264, Mannheim, Germany). For quantitative PCR, the LightCycler system offers the advantage of fast and real-time measurement of fluorescent signals during amplification. The housekeeping gene α-enolase was used as internal reference to normalize the RNA levels of the genes being studied.

Following primers were used:

IL-8 5′ primer	5′-ATG ACT TCC AAG CTG GCC GTG GCT-3′
IL-8 3′ primer	5′-TCT CAG CCC TCT TCA AAA ACT TCT C-3′
IL-6 5′ primer	5′-ATG AAC TCC TTC TCC ACA AGC-3′
IL-6 3′ primer	5′-CTA CAT TTG CCG AAG AGC CCT CAG GCT GGA CTG-3′
HO-1 5′ primer	5′-AAC TGT CGC CAC CAG AAA GCT GAG-3′
HO-1 3′ primer	5′-AAG ATT GCC CAG AAA GCC CTG GAC-3′
α-enolase 5′ primer	5′-GTT AGC AAG AAA CTG AAC GTC ACA–3′
α-enolase 3′ primer	5′-TGA AGG ACT TGT ACA GGT CAG-3′

2.9. Statistical analysis

For statistical analysis of the data, we used the Student's *t*-test. Results are given as mean values ± SD.

3. Results and discussion

3.1. Deposition and particle size distribution

The spatial uniformity and the dose of the deposited ufp was examined with C-ufp generated as described above. For this experiment, we supplied C-ufp at a concentration of $7 \times 10^6\ cm^{-3}$ (count median diameter CMD = 90 nm) for 3 h at the prescribed flow rate of 250 ml min^{-1}. The deposition pattern was determined by placing 10 × 10 mm quartz plates for subsequent scanning electron microscopy (SEM) analysis at several positions across the filter membrane. As seen from Fig. 2, the C-ufp display a soot-like

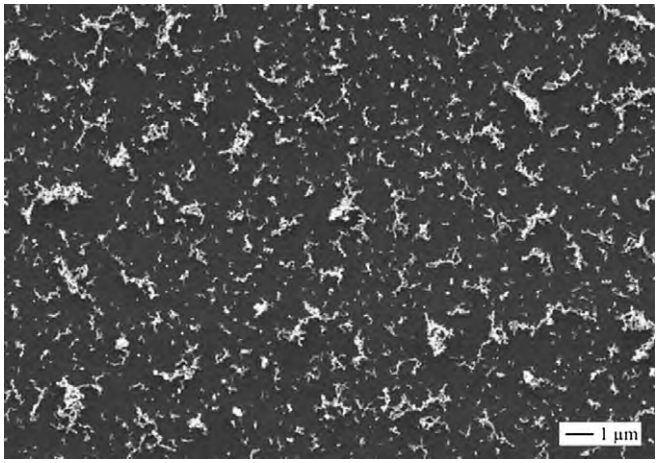

Fig. 2. Spatially uniform distribution of deposited ultrafine carbon particles obtained by placing quartz plates into the stagnation point flow within the exposure chamber.

structure, i.e., they appear as agglomerates consisting of numerous primary spheres. As shown by Tippe et al. (2002) particle agglomeration on the quartz plates is not significant. Fig. 2 shows that the deposition pattern appears spatially uniform in all directions. Due to flow disturbances near the outer rim of the filter the uniform regime is limited to 40 mm of the 47 mm filter. In addition, quantitative analysis of the SEM grids showed that 2% of the incoming particles were deposited onto the filter. This value is consistent with the theoretical and experimental analysis of the original (smaller) version of the chamber as described by Tippe et al. (2002). Hence, as expected from Reynolds-invariant scaling, we conclude that the present version of the exposure chamber has the same performance characteristics as the original chamber, i.e., 75–1000 nm particles are deposited spatially uniform across the filter and at a constant deposition efficiency of 2% (Tippe et al., 2002).

To validate the applicability of this chamber for ALI cell exposure experiments we performed an initial study with A549 epithelial cells as described above. For these experiments, the particle size distribution of the C-ufp was measured upstream of the humidifiers and at the chamber outlet. Before humidification, the count median diameter (CMD) in a representative experiment was 90 ± 2 nm ($\sigma_g = 1.55$) at a number concentration of $(1.9 \pm 0.2) \times 10^6$ cm^{-3}. There was a slight but detectable decrease of particle concentration from $(1.9 \pm 0.2) \times 10^6$ cm^{-3} to $(1.3 \pm 0.1) \times 10^6$ cm^{-3} and an increase of particle CMD from 90 ± 2 nm ($\sigma_g = 1.55$) to 105 ± 2 nm ($\sigma_g = 1.53$) between upstream and downstream location (Fig. 3). This was due to particle losses and agglomeration when passing the exposure system during a residence time of 50–60 s. For all measurements, the residence time in the SMPS and the connecting tubes in front of the SMPS was around 10 s. Since the downstream location of the SMPS was much closer to the exposure chamber than the upstream location, we used the integral of these size distributions to infer the deposited aerosol dose. For a deposition rate of 2%, a volumetric flow rate of 250 ml min^{-1}, a mean particle density of 0.3 g cm^{-3} and an exposure time of 6 h, the total deposited aerosol mass was 44 ± 4 ng cm^{-2} (low dose), 87 ± 23 ng cm^{-2} (mid dose) and 230 ± 70 ng cm^{-2} (high dose). The mean effective particle density was determined from Eqs. (3) and (4) in Maricq and Xu (2004) using a fractal dimension of 2, an effective primary diameter of 7.5 nm (assumed equal to the primary diameter determined by the SEM) and primary particle density of 2 g cm^{-3} (Wentzel et al., 2003; Roth et al., 2004).

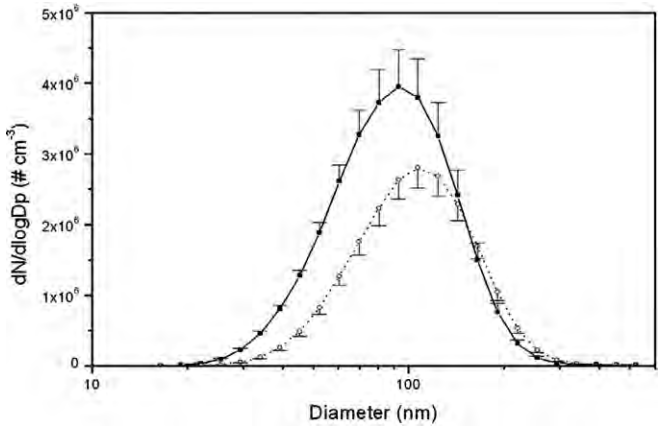

Fig. 3. Typical size distributions of the ultrafine carbonaceous particles at the inlet of the humidifier (black squares) and the outlet of the exposure chamber (open circles; $n \geqslant 24$).

We add as caveat, that a substantial fraction of the particles in Fig. 2 appears to be considerably larger than the reported CMD of about 100 nm. This is a result of two effects. First, Fig. 2 was taken at more than twice the highest dose used for cell exposure experiments, i.e., the distances between the sites of particle deposition are reduced and the probability of particle superposition on the substrate is enhanced. Secondly, the low resolution necessary to show the uniform deposition pattern over a wide viewing window cannot resolve particles deposited in close proximity. However, the detailed SEM analysis performed by Tippe et al. (2002) with the same kind of challenge aerosol confirmed the CMD of about 100 nm, i.e. agglomeration did not occur at a significant rate. Finally we note, that we cannot rule out some particle agglomeration due to flocculation on the liquid layer covering the cell cultures. However, this issue is expected to be even more pronounced for submerse exposure systems.

3.2. A549 monolayer: integrity and cell viability

Confocal laser scanning microscopy showed that nearly tight monolayers of A549 cells grown on Anodisc membranes were obtained after 10 days of submersed cultures (data not shown). We next determined cell viability by the WST-1 assay. Compared to submersed cultured cell monolayers as control, we found $93.7 \pm 9.1\%$ viability after 6 h exposure to clean air and $94.9 \pm 9.5\%$ viability after 6 h low, mid and high dose aerosol exposure ($n = 13$). Hence, there is no indication for toxic effects due to aerosol exposure even for the highest dose.

3.3. Gene expression profiles in absence of particles (clean air control)

There was a 2- to 3-fold increase of IL-8 and IL-6 transcription after 6 h exposure at the ALI with clean air compared to the submersed control (Fig. 4A), which indicates a weak stress solely induced by the air flow. Importantly, subsequent activation by TNF as a biological stimulus did not induce an altered response versus the submersed control, indicating that cell integrity was not affected under these exposure conditions (Fig. 4B). Furthermore, we found an increased transcription of HO-1 in the ALI culture after exposure with clean air compared with submersed cultures (Fig. 4A) and this response was barely altered after TNF post-stimulation (Fig. 4B). The inability of TNF to upregulate HO-1 expression in A549 cells was recently reported (Bundy et al., 2005).

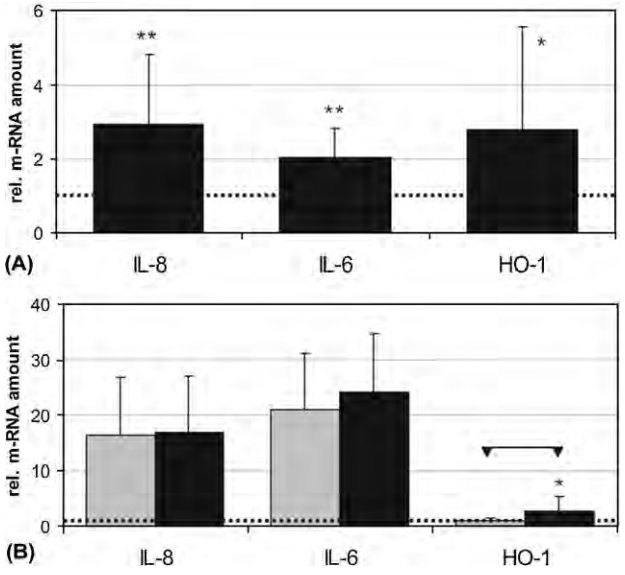

Fig. 4. ALI exposure of epithelial cell monolayers to clean air: (A) transcription of IL-8, IL-6 and HO-1 after clean air exposure of cells versus untreated cells in submersed cultures (dotted line, $n = 15$). $^{**}p \leqslant 0.01$, $^{*}p \leqslant 0.05$; (B) transcription of IL-8, IL-6 and HO-1 after TNF stimulation of cells in submersed cultures (grey bars, $n = 15$) and after TNF post-stimulation of clean air exposed cells (black bars, $n = 15$) versus cells in submersed culture without TNF stimulation (dotted line, $n = 15$). TNF stimulation indicates the ability of cells to respond to a strong inflammatory stimulus.

3.4. Responses of cells after exposure to ufp at the ALI

ALI-exposure to $(1.8 \pm 0.2) \times 10^6$ cm^{-3} ufp for 6 h resulted in the deposition of $(2.6 \pm 0.3) \times 10^8$ cm^{-2} particles corresponding to 87 ± 23 ng cm^{-2} membrane surface (mid dose, $n = 6$), assuming a particle density of 0.3 g cm^{-3}. Following these exposures, transcription of IL-8 and IL-6 was not different from the clean air control. Similarly, the TNF-induced increase in gene transcription was hardly influenced by a preceding particle exposure (Fig. 5A). Transcription of the antioxidant enzyme HO-1 was significantly increased (2.7-fold) after exposure to ufp in the mid dose range. By contrast, low or high dose exposure to particles had no effect on HO-1 transcription (Fig. 5B). It is supposed that the absence of HO-1 stimulation at high-dose particle exposure might reflect an early onset of a cytotoxic response, which is below the sensitivity level of the WST-1 viability assay. Several studies have demonstrated the upregulation of HO-1 by particulate matter in submersed cultures and its relation to enhanced oxidative stress in macrophages, endothelial and epithelial cells (Li et al., 2000, 2003; Chin et al., 2003) or in whole lung tissue of mice after inhalation (Risom et al., 2003). The transcription rates of HO-1 might be a sensitive tool for the cell to regulate between anti-oxidative protection systems after mild oxidative stress and pro-inflammatory pathways leading to cell death after strong oxidative stress at higher exposure levels as discussed by Li et al. (2002) in their stratified oxidative stress model.

The dose of airborne particles to induce an increased HO-1 expression in the target cells was much lower than

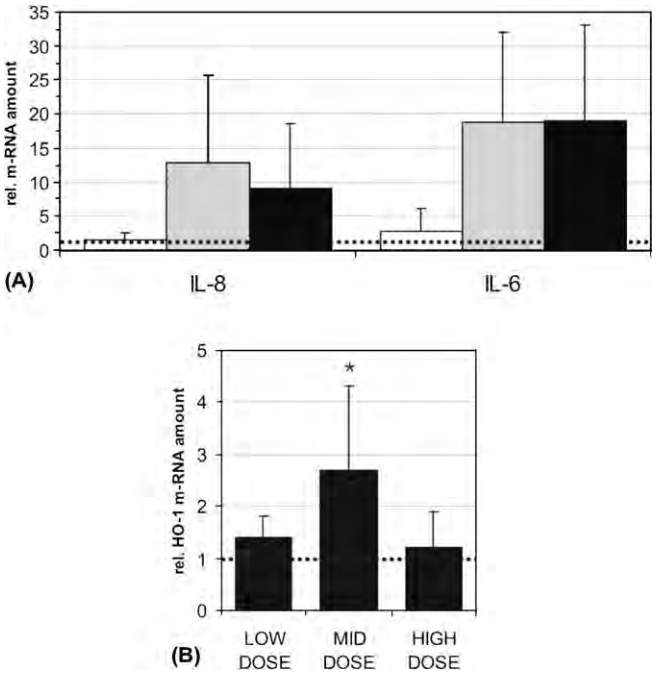

Fig. 5. ALI exposure of epithelial cell monolayers to ufp: (A) transcription of IL-8 and IL-6 after exposure under mid dose conditions to ufp (white bars), after TNF post-stimulation of ufp exposed cells (grey bars) and after TNF post-stimulation of clean air exposed cells (black bars) compared to clean air exposed cells as control (dotted line, $n = 6$). TNF post-stimulation indicates the ability of cells to respond to a strong inflammatory stimulus; (B) transcription of HO-1 after exposure to ufp compared to clean air exposed cells. Low dose $= 44 \pm 4$ ng, mid dose $= 87 \pm 23$ ng and high dose $= 230 \pm 70$ ng deposited particles during 6 h of exposure on 1 cm^2 of cell monolayer surface (density $= 0.3$ g cm^{-3}; $n = 4$–6). $^{*}p \leqslant 0.05$.

that of suspended particles to induce a similar effect in submersed exposures (data not shown), indicating a substantially higher sensitivity.

4. Conclusions

We described, tested and applied a novel experimental system to expose three 40 mm membrane dishes with cells (3×10^7 cells) at the air–liquid interface (ALI) to particles between 75 and 1000 nm. The main strengths of this device are the spatially uniform particle deposition pattern and the well-defined dose (2% of the airborne particles are deposited) that can be determined from the continuously monitored particle size distribution. Both aspects are essential to consider dose–response relationships with aerosols. Further strengths are the life-like exposure conditions and the remarkably high sensitivity of ALI exposures compared to submersed exposures in detecting particle responses.

The biological validation experiment performed here showed that significant upregulation of HO-1 transcription after exposure to an accumulated dose of 87 ng carbonaceous ufp per cm^2 of nearly confluent A549 target cells. This demonstrates a highly sensitive antioxidant and stress response.

References

Abe, S., Takizawa, H., Sugawara, I., Kudoh, S., 2000. Diesel exhaust (DE)-induced cytokine expression in human bronchial epithelial cells: a study with a new cell exposure system to freshly generated DE in vitro. Am. J. Respir. Cell Mol. Biol. 22, 296–303.

Aufderheide, M., Ritter, D., Knebel, J.W., Scherer, G., 2001. A method for in vitro analysis of the biological activity of complex mixtures such as sidestream cigarette smoke. Exp. Toxicol. Pathol. 53, 141–152.

Bayram, H., Devalia, J.L., Sapsford, R.J., Ohtoshi, T., Miyabara, Y., Sagai, M., Davies, R.J., 1998. The effect of diesel exhaust particles on cell function and release of inflammatory mediators from human bronchial epithelial cells in vitro. Am. J. Respir. Cell Mol. Biol. 18, 441–448.

Beck-Speier, I., Dayal, N., Karg, E., Maier, K.L., Schumann, G., Schulz, H., Semmler, M., Takenaka, S., Stettmaier, K., Bors, W., Ghio, A., Samet, J.M., Heyder, J., 2005. Oxidative stress and lipid mediators induced in alveolar macrophages by ultrafine particles. Free Radic. Biol. Med. 38, 1080–1092.

Brunauer, S., Emmett, P.H., Teller, E., 1938. Adsorption of gases in multimolecular layers. J. Am. Chem. Soc. 60, 309–319.

Bundy, R.E., Hoare, G.S., Kite, A., Beach, J., Yacoub, M., Marczin, N., 2005. Redox regulation of p38 MAPK activation and expression of ICAM-1 and heme oxygenase-1 in human alveolar epithelial (A549) cells. Antioxid. Redox Sign. 7, 14–24.

Cheng, M.D., Malone, B., Storey, J.M., 2003. Monitoring cellular responses of engine-emitted particles by using a direct air–cell interface deposition technique. Chemosphere 53, 237–243.

Chin, B.Y., Trush, M.A., Choi, A.M., Risby, T.H., 2003. Transcriptional regulation of the HO-1 gene in cultured macrophages exposed to model airborne particulate matter. Am. J. Physiol. Lung Cell Mol. Physiol. 284, L473–L480.

Choi, J.H., Kim, J.S., Kim, Y.C., Kim, Y.S., Chung, N.H., Cho, M.H., 2004. Comparative study of PM2.5- and PM10-induced oxidative stress in rat lung epithelial cells. J. Vet. Sci. 5, 11–18.

Cook, J.A., Mitchell, J.B., 1989. Viability measurements in mammalian cell systems. Anal. Biochem. 179, 1–7.

Donaldson, K., Brown, D., Clouter, A., Duffin, R., MacNee, W., Renwick, L., Tran, L., Stone, V., 2002. The pulmonary toxicology of ultrafine particles. J. Aerosol Med. 15, 213–220.

Ferron, G.A., Haider, B., Kreyling, W., 1985. A method for the approximation of the relative humidity in the upper human airways. Math. Biol. 47, 565–589.

Foster, K.A., Oster, C.G., Mayer, M.M., Avery, M.L., Audus, K.L., 1998. Characterization of the A549 cell line as a type II pulmonary epithelial cell model for drug metabolism. Exp. Cell Res. 243, 359–366.

Foster, K.A., Yazdanian, M., Audus, K.L., 2001. Microparticulate uptake mechanisms of in vitro cell culture models of the respiratory epithelium. J. Pharm. Pharmacol. 53, 57–66.

Griese, M., Reinhardt, D., 1998. Smaller sized particles are preferentially taken up by alveolar type II pneumocytes. J. Drug Target. 5, 471–479.

Hofer, T.P., Bitterle, E., Beck-Speier, I., Maier, K.L., Frankenberger, M., Heyder, J., Ziegler-Heitbrock, L., 2004. Diesel exhaust particles increase LPS-stimulated COX-2 expression and PGE2 production in human monocytes. J. Leukoc. Biol. 75, 856–864.

Kim, K.J., Borok, Z., Crandall, E.D., 2001. A useful in vitro model for transport studies of alveolar epithelial barrier. Pharm. Res. 18, 253–255.

Knebel, J.W., Ritter, D., Aufderheide, M., 1998. Development of an in vitro system for studying effects of native and photochemically transformed gaseous compounds using an air/liquid culture technique. Toxicol. Lett. 96–97, 1–11.

Li, N., Venkatesan, M.I., Miguel, A., Kaplan, R., Gujuluva, C., Alam, J., Nel, A., 2000. Induction of heme oxygenase-1 expression in macrophages by diesel exhaust particle chemicals and quinones via the antioxidant-responsive element. J. Immunol. 165, 3393–3401.

Li, N., Kim, S., Wang, M., Froines, J., Sioutas, C., Nel, A., 2002. Use of a stratified oxidative stress model to study the biological effects of ambient concentrated and diesel exhaust particulate matter. Inhal. Toxicol. 14, 459–486.

Li, N., Hao, M., Phalen, R.F., Hinds, W.C., Nel, A.E., 2003. Particulate air pollutants and asthma. A paradigm for the role of oxidative stress in PM-induced adverse health effects. Clin. Immunol. 109, 250–265.

Maricq, M.M., Xu, N., 2004. The effective density and fractal dimension of soot particles from premixed flames and motor vehicle exhaust. J. Aerosol Sci. 35, 1251–1274.

Oberdorster, G., Finkelstein, J.N., Johnston, C., Gelein, R., Cox, C., Baggs, R., Elder, A.C., 2000. Acute pulmonary effects of ultrafine particles in rats and mice. Res. Rep. Health Eff. Inst. 5–74, disc 75–86.

Peters, A., Wichmann, H.E., Tuch, T., Heinrich, J., Heyder, J., 1997. Respiratory effects are associated with the number of ultrafine particles. Am. J. Respir. Crit. Care Med. 155, 1376–1383.

Reibman, J., Hsu, Y., Chen, L.C., Kumar, A., Su, W.C., Choy, W., Talbot, A., Gordon, T., 2002. Size fractions of ambient particulate matter induce granulocyte macrophage colony-stimulating factor in human bronchial epithelial cells by mitogen-activated protein kinase pathways. Am. J. Respir. Cell Mol. Biol. 27, 455–462.

Renwick, L.C., Brown, D., Clouter, A., Donaldson, K., 2004. Increased inflammation and altered macrophage chemotactic responses caused by two ultrafine particle types. Occup. Environ. Med. 61, 442–447.

Risom, L., Dybdahl, M., Bornholdt, J., Vogel, U., Wallin, H., Moller, P., Loft, S., 2003. Oxidative DNA damage and defence gene expression in the mouse lung after short-term exposure to diesel exhaust particles by inhalation. Carcinogenesis 24, 1847–1852.

Ritter, D., Knebel, J.W., Aufderheide, M., 2001. In vitro exposure of isolated cells to native gaseous compounds–development and validation of an optimized system for human lung cells. Exp. Toxicol. Pathol. 53, 373–386.

Ritter, D., Knebel, J.W., Aufderheide, M., 2003. Exposure of human lung cells to inhalable substances: a novel test strategy involving clean air exposure periods using whole diluted cigarette mainstream smoke. Inhal. Toxicol. 15, 67–84.

Roth, C., Ferron, G.A., Karg, E., Lentner, B., Schumann, G., Takenaka, S., Heyder, J., 2004. Generation of Ultrafine Particles by Spark Discharging. Aerosol Sci. Technol. 38, 228–235.

Rothen-Rutishauser, B., Kapp, N., Schuerch, S., Geiser, M., Gehr, P., 2004. Red Blood cells as a model for non-phagocytic cells to study the non-specific uptake of ultrafine particles in the lung. Abstracts of ERS-Meeting 2004 in Glasgow. Eur. Respir. J. 24 (Suppl. 48), 552s.

Rothen-Rutishauser, B.M., Kiama, S.G., Gehr, P., 2005. A three-dimensional cellular model of the human respiratory tract to study the interaction with particles. Am. J. Respir. Cell Mol. Biol. 32, 281–289.

Stearns, R., Paulauskis, J., Godleski, J., 2001. Endocytosis of ultrafine particles by A549 cells. Am. J. Respir. Cell Mol. Biol. 24, 108–115.

Tippe, A., Heinzmann, U., Roth, C., 2002. Deposition of fine and ultrafine aerosol particles during exposure at the air/cell interface. J. Aerosol Sci. 33, 207–218.

Wang, A.M., Doyle, M.V., Mark, D.F., 1989. Quantitation of mRNA by the polymerase chain reaction. Proc. Natl. Acad. Sci. USA 86, 9717–9721.

Wentzel, M., Gorzawski, H., Naumann, K.-H., Saathoff, H., Weinbruch, S., 2003. Transmission electron microscopical and aerosol dynamical characterization of soot aerosols. J. Aerosol Sci. 34, 1347–1370.

Wottrich, R., Diabate, S., Krug, H.F., 2004. Biological effects of ultrafine model particles in human macrophages and epithelial cells in mono- and co-culture. Int. J. Hyg. Environ. Health 207, 353–361.